

## INVESTIGATING THE IMPACT OF POROSITY DISTRIBUTION AND GRADING PARAMETER ON THE FREE VIBRATION OF FUNCTIONALLY GRADED BEAMS

Lazreg Hadji<sup>1</sup>, Vagelis Plevris<sup>2</sup> and Royal Madan<sup>3</sup>

<sup>1</sup> Department of Civil Engineering, University of Tiaret  
BP 78 Zaaroura, Tiaret 14000 Tiaret, Algeria  
e-mail: [lazreg.hadji@univ-tiaret.dz](mailto:lazreg.hadji@univ-tiaret.dz)

<sup>2</sup> Department of Civil and Architectural Engineering, Qatar University  
Doha P.O. Box 2713, Qatar  
e-mail: [vplevris@qu.edu.qa](mailto:vplevris@qu.edu.qa)

<sup>3</sup> Department of Mechanical Engineering, G H Raisoni Institute of Engineering and Technology,  
Nagpur 440016, India  
e-mail: [royalmadan6293@gmail.com](mailto:royalmadan6293@gmail.com)

---

### Abstract

*This study focuses on investigating the free vibration of porous functionally graded (FG) beams and the impact of porosity distribution on the properties and performance of materials. To achieve this, the study assumes that the beam's material characteristics vary continuously along its thickness direction. The volume fraction of constituents is specified using the modified rule of the mixture, which includes porosity volume fraction with changed porosity patterns across the cross-section. The study uses the hyperbolic shear deformation theory without shear correction factors to derive the equations of motion by applying Hamilton's principle. The study employs Navier's method to obtain analytical results for the free vibration of porous/non-porous FG beams under simply supported boundary conditions at both ends. To verify the proposed formulation, the study compares the results with relevant findings from the literature. The study also examines the relationship between frequency of vibration and grading parameter in homogeneous porosity distributions, as well as the frequency of vibration in beam structures with different porosity patterns. Additionally, numerical examples are provided to investigate the impact of parameters like power-law index, span to depth ratio, porosity distribution pattern, and porosity volume fraction on the natural frequencies of FG beams. The analysis provides significant insights into the behavior of different porous materials and can be useful for designing and selecting materials with porosities.*

**Keywords:** Free Vibration, Functionally Graded Materials, Porosity, Hyperbolic Shear Deformation Theory, Navier Solution.

## 1 INTRODUCTION

Composite materials are materials that are made up of two or more different materials that are combined together to form a single material with unique properties. The different materials used in a composite material are called constituents, and they can be selected based on their specific properties, such as strength, stiffness, durability, and others. In most cases, composites exhibit consistent material properties throughout their structure, meaning that the properties do not change significantly in any direction [1]. On the other hand, functionally graded materials (FGMs) are advanced materials that have a continuously varying composition or structure, typically from one end of the material to the other. This variation can be controlled to produce specific functional properties in different regions of the material. FGMs are typically designed to have properties that vary gradually from one region to another, rather than abruptly changing at a boundary. This gradual change in properties can result in improved performance and durability compared to homogeneous materials, making them more suitable for applications where the properties of the material need to vary to achieve optimal performance [2]. To prevent delamination caused by differences in thermo-mechanical properties, FGMs are fabricated in a way that ensures a gradual transition of material properties from one layer to another. This gradual transition helps to reduce the mismatch in the thermal expansion coefficients of different layers and minimizes the formation of interfacial stresses that can cause delamination [3].

The differential quadrature method (DQM), a numerical method used to approximate the solution of differential equations, was used to calculate the frequencies of FG plates with different boundary conditions (BCs) [4]. This technique was later applied to other studies, such as analyzing the free vibration of micro circular plates under thermal loads and 3D free vibration analysis [5, 6]. In the work of Alipour et al. [7], the free vibration behavior of 2D FGMs under various boundary conditions was investigated. The authors found that clamped boundary conditions resulted in the highest frequency, simply supported conditions resulted in the lowest frequency, and free-free conditions resulted in intermediate frequencies. Nie and Batra [8] used a semi-analytical numerical method to analyze the bending behavior of 2D FG circular and annular plates and the bending and thermal deformations of FG beams with various end conditions. Additionally, an impact analysis using a similar numerical method was performed [9].

The distribution of porosity in a structure can be uniform or non-uniform depending on how it is fabricated. To avoid negative effects on performance, researchers are exploring ways to eliminate porosity [10]. Pores may form in powder metallurgy due to improper sintering and different reinforcement shapes, with irregular shapes leading to more pores than rounded or elliptical ones. The elastic modulus of a material also depends on the reinforcement shape, with spherical particles having the highest elastic modulus. Improper solidification during centrifugal casting and rapid heating and solidification during additive manufacturing may also lead to porosity, as noted in several studies [11-14].

The free vibration behavior of functionally graded beams was investigated by utilizing the finite element method. The findings suggest that alterations in material distribution along the axial direction can affect the stiffness of the beam, leading to changes in mode shapes and frequencies. The fundamental frequencies and mode shapes were not impacted by the slenderness ratio due to the limitations of the Euler-beam theory. Moreover, the natural frequencies either increased or decreased with a change in the power exponent, depending on the material distribution [15]. Apart from these, various methods have been employed by researchers to study the free vibration of FG beams such as dynamic stiffness method [16], Rayleigh–Ritz method [17], higher-order shear deformation beam theories [18], among others.

A detailed dynamic analysis of a functionally graded beam can pose significant computational challenges [19]. In a previous work, the authors attempted a static and free vibration

analysis of porous FG beams [20]. The main objective of the present research work is to investigate how the distribution of voids affects the free vibration characteristics of FGM beams by utilizing an advanced shear deformation model. This model takes into account the impact of voids by employing a modified mixture law that incorporates void phases introduced by previous studies from [21, 22]. The study also investigates the effects of various parameters on the free vibration of FGM beams. These parameters include the power index, pore volume fraction (amount and distribution of voids or pores), geometry ratio (dimensions of the FGM beam), porosity distribution pattern, and thickness ratio. By studying the effects of these parameters, the study aims to understand the behavior of FGM beams under free vibration conditions. The variation of material properties in the FGM beam is assumed to follow a power-law distribution of the volume fraction of the constituents. To derive the equation of motion for FGM beams, Hamilton's principle is used. The results of the study can be useful in designing FGM structures that results in higher frequency.

## 2 GEOMETRIC CONFIGURATION AND MATERIAL PROPERTIES

An FG beam is considered with geometry dimensions as shown in Figure 1. The material properties vary in a graded manner in the thickness direction (along  $h$ ). In this study, we investigate an imperfect functionally graded beam that contains a specific volume fraction of porosity  $\alpha$  ( $\alpha \ll 1$ ), which is distributed differently between the metal (denoted as  $m$ ) and ceramic ( $c$ ) components. To account for this porosity distribution, we utilize the modified mixture rule developed by Wattanasakulpong and Ungbhakorn [23].

$$P(z) = P_m \left( V_m - \frac{\alpha}{2} \right) + P_c \left( V_c - \frac{\alpha}{2} \right) \quad (1)$$

The assumed relationship for the volume fraction of ceramic is a power law, as shown below:

$$V_c = \left( \frac{z}{h} + \frac{1}{2} \right)^k \quad (2)$$

The relation obtained can be written as:

$$P(z) = (P_c - P_m) \left( \frac{z}{h} + \frac{1}{2} \right)^k + P_m - (P_c + P_m) \frac{\alpha}{2} \quad (3)$$

where  $k$  is the power law index. The FGM beam can transform into a fully ceramic or fully metal beam, depending on the value of  $k$ . If  $k$  is zero, then the beam is fully ceramic, while for large values of  $k$ , it becomes fully metal. The elastic modulus  $E$  for porous FG plate can be written as [24, 25].

$$E(z) = (E_c - E_m) \left( \frac{z}{h} + \frac{1}{2} \right)^k + E_m - (E_c + E_m) \frac{\alpha}{2} \quad (4)$$

To determine the material properties of a perfect functionally graded beam, the volume fraction of porosity,  $\alpha$ , is assumed to be zero. Since the Poisson ratio,  $\nu$ , only varies slightly, it can be considered constant. The current study investigates various forms of porosity, including the patterns "O", "V", and "X", as shown in detail in Table 1.

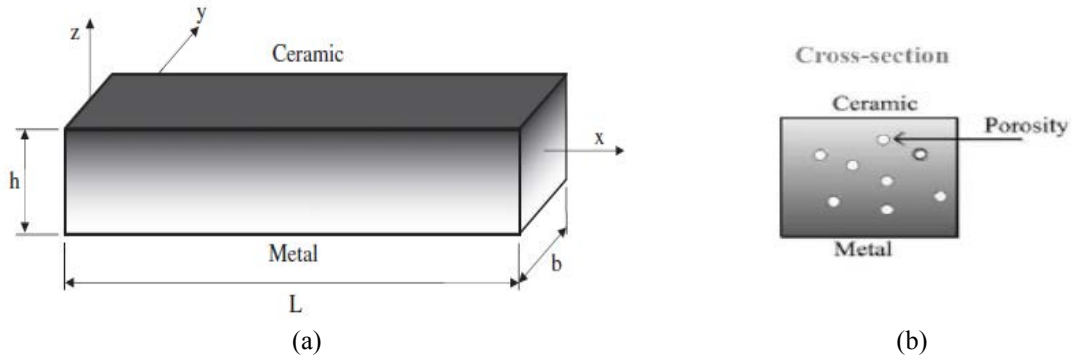


Figure 1. Geometry of the FG beam: (a) 3D view, (b) Cross section.

### 3 KINEMATIC, STRAIN AND STRESS RELATIONS

The displacement field of the present higher order shear deformation model is given by the following expression [26]:

$$u(x, z, t) = u_0(x, t) - z \frac{\partial w_b}{\partial x} - f(z) \frac{\partial w_s}{\partial x} \quad (5)$$

$$w(x, z, t) = w_b(x, t) + w_s(x, t) \quad (6)$$

The study uses a refined shear deformation theory where the axial displacement of a point on the mid-plane of the beam is represented by  $u_0$ , and the bending and shear components of transverse displacement are  $w_b$  and  $w_s$ , respectively. The theory employs a shape function,  $f(z)$ , to determine the distribution of transverse shear strain and shear stress throughout the beam depth, while satisfying stress-free boundary conditions.

$$f(z) = z \left[ 1 + \frac{3\pi}{2} \operatorname{sech} \left( \frac{1}{2} \right)^2 \right] - \frac{3\pi}{2} h \tanh \left( \frac{z}{h} \right) \quad (7)$$

The strains associated with the displacements in Eqs (5) and (6) are

$$\varepsilon_x = \varepsilon_x^0 + z k_x^b + f(z) k_x^s \quad (8)$$

$$\gamma_{xz} = g(z) \gamma_{xz}^s \quad (9)$$

where

$$\varepsilon_x^0 = \frac{\partial u_0}{\partial x}, \quad k_x^b = -\frac{\partial^2 w_b}{\partial x^2}, \quad \gamma_{xz}^s = \frac{\partial w_s}{\partial x} \quad (10)$$

$$g(z) = 1 - f'(z) \quad \text{and} \quad f'(z) = \frac{df(z)}{dz} \quad (11)$$

The generalized Hooke's law expresses the state of stress present in the beam in the following manner:

$$\sigma_x = Q_{11}(z) \varepsilon_x \quad \text{and} \quad \tau_{xz} = Q_{55}(z) \gamma_{xz} \quad (12)$$

where

$$Q_{11}(z) = E(z) \quad \text{and} \quad Q_{55}(z) = \frac{E(z)}{2(1+\nu)} \quad (13)$$

#### 4 EQUATIONS OF MOTION

In order to obtain the equations of motion, the method of Hamilton's principle is applied, as shown in the following equation [27].

$$\delta \int_{t_1}^{t_2} (U - T) dt = 0 \quad (14)$$

The variables used in this equation are the time,  $t$ , the time instances  $t_1, t_2$ , representing the initial and final times, respectively, the potential strain energy,  $U$ , and the kinetic energy,  $T$ . The strain energy variation of the beam can be expressed as:

$$\begin{aligned} \delta U = \int_0^L \int_{-\frac{h}{2}}^{\frac{h}{2}} (\sigma_x \delta \varepsilon_x + \tau_{xz} \delta \gamma_{xz}) dz dx = \\ \int_0^L \left( N \frac{d\delta u_0}{dx} - M_b \frac{d^2\delta w_b}{dx^2} - M_s \frac{d^2\delta w_s}{dx^2} + Q \frac{d\delta w_s}{dx} \right) dx \end{aligned} \quad (15)$$

where  $N_x, M_b, M_s$  and  $Q_{xz}$  are the stress resultants defined as

$$(N, M_b, M_s) = \int_{-h/2}^{h/2} (1, z, f) \sigma_x dz \quad \text{and} \quad Q_{xz} = \int_{-h/2}^{h/2} g \tau_{xz} dz \quad (16)$$

The change in the kinetic energy can be stated as:

$$\begin{aligned} \delta T = \int_0^L \int_{-h/2}^{h/2} \rho(z) [\dot{u} \delta \dot{u} + \dot{w} \delta \dot{w}] dz dx = \\ \int_0^L \left\{ I_1 \left[ \dot{u}_0 \delta \dot{u}_0 + (\dot{w}_b + \dot{w}_s) (\delta \dot{w}_b + \delta \dot{w}_s) \right] - I_2 \left( \dot{u}_0 \frac{d\delta \dot{w}_b}{dx} + \frac{d\dot{w}_b}{dx} \delta \dot{u}_0 \right) \right. \\ \left. + I_4 \left( \frac{d\dot{w}_b}{dx} \frac{d\delta \dot{w}_b}{dx} \right) - I_3 \left( \dot{u}_0 \frac{d\delta \dot{w}_s}{dx} + \frac{d\dot{w}_s}{dx} \delta \dot{u}_0 \right) + I_6 \left( \frac{d\dot{w}_s}{dx} \frac{d\delta \dot{w}_s}{dx} \right) \right. \\ \left. + I_5 \left( \frac{d\dot{w}_b}{dx} \frac{d\delta \dot{w}_s}{dx} + \frac{d\dot{w}_s}{dx} \frac{d\delta \dot{w}_b}{dx} \right) \right\} dx \end{aligned} \quad (17)$$

where the dot-superscript convention indicates the differentiation with respect to the time variable  $t$ ;  $\rho(z)$  is the mass density; and  $(I_1, I_2, I_3, I_4, I_5, I_6)$  are the mass inertias defined as

$$(I_1, I_2, I_3, I_4, I_5, I_6) = \int_{-h/2}^{h/2} (1, z, f, z^2, zf, f^2) \rho(z) dz \quad (18)$$

By plugging in the equations for  $\delta U$  and  $\delta T$  from Eqs (15) and (17) into Eq. (14), and performing integration by parts with respect to both spatial and temporal variables, while grouping together the coefficients of  $\delta u_0, \delta w_b$ , and  $\delta w_s$ , we can obtain the equations of motion for the functionally graded beam:

$$\delta u_0 : \frac{dN_x}{dx} = I_1 \ddot{u}_0 - I_2 \frac{d\ddot{w}_b}{dx} - I_3 \frac{d\ddot{w}_s}{dx} \tag{19}$$

$$\delta w_b : \frac{d^2 M_b}{dx^2} = I_1 (\ddot{w}_b + \ddot{w}_s) + I_2 \frac{d\ddot{u}_0}{dx} - I_4 \frac{d^2 \ddot{w}_b}{dx^2} - I_5 \frac{d^2 \ddot{w}_s}{dx^2} \tag{20}$$

$$\delta w_s : \frac{d^2 M_s}{dx^2} + \frac{dQ_{xz}}{dx} = I_1 (\ddot{w}_b + \ddot{w}_s) + I_3 \frac{d\ddot{u}_0}{dx} - I_5 \frac{d^2 \ddot{w}_b}{dx^2} - I_6 \frac{d^2 \ddot{w}_s}{dx^2} \tag{21}$$

The equations of motion in relation to the displacement can be obtained by replacing the stress resultants from Eq. (16) into Eqs (19), (20), (21) ( $u_0, w_b, w_s$ ) as follows:

$$A_{11} \frac{\partial^2 u_0}{\partial x^2} - B_{11} \frac{\partial^3 w_b}{\partial x^3} - B_{11}^s \frac{\partial^3 w_s}{\partial x^3} = I_1 \ddot{u}_0 - I_2 \frac{d\ddot{w}_b}{dx} - I_3 \frac{d\ddot{w}_s}{dx} \tag{22}$$

$$B_{11} \frac{\partial^3 u_0}{\partial x^3} - D_{11} \frac{\partial^4 w_b}{\partial x^4} - D_{11}^s \frac{\partial^4 w_s}{\partial x^4} = I_1 (\ddot{w}_b + \ddot{w}_s) + I_2 \frac{d\ddot{u}_0}{dx} - I_4 \frac{d^2 \ddot{w}_b}{dx^2} - I_5 \frac{d^2 \ddot{w}_s}{dx^2} \tag{23}$$

$$B_{11}^s \frac{\partial^3 u_0}{\partial x^3} - D_{11}^s \frac{\partial^4 w_b}{\partial x^4} - H_{11}^s \frac{\partial^4 w_s}{\partial x^4} + A_{55}^s \frac{\partial^2 w_s}{\partial x^2} = I_1 (\ddot{w}_b + \ddot{w}_s) + I_3 \frac{d\ddot{u}_0}{dx} - I_5 \frac{d^2 \ddot{w}_b}{dx^2} - I_6 \frac{d^2 \ddot{w}_s}{dx^2} \tag{24}$$

where the terms  $A_{11}, D_{11}$ , etc., denote the beam stiffness, defined by

$$(A_{11}, B_{11}, D_{11}, B_{11}^s, D_{11}^s, H_{11}^s) = \int_{-h/2}^{h/2} Q_{11} (1, z, z^2, f(z), z f(z), f^2(z)) dz \tag{25}$$

$$A_{55}^s = \int_{-h/2}^{h/2} Q_{55} [g(z)]^2 dz \tag{26}$$

### 5 ANALYTICAL SOLUTION

Assuming certain variations, the variables  $u_0, w_b, w_s$  can be expressed, and these equations of motion can lead to Navier solutions for simply supported beams.

$$\begin{Bmatrix} u_0 \\ w_b \\ w_s \end{Bmatrix} = \sum_{m=1}^{\infty} \begin{Bmatrix} U_m \cdot \cos(\lambda x) \cdot e^{i\omega t} \\ W_{bm} \cdot \sin(\lambda x) \cdot e^{i\omega t} \\ W_{sm} \cdot \sin(\lambda x) \cdot e^{i\omega t} \end{Bmatrix} \tag{27}$$

Here,  $U_m, W_{bm}$ , and  $W_{sm}$  are undetermined parameters that need to be calculated, while  $\omega$  represents the eigenfrequency corresponding to the eigenmode. By substituting the expansions of Eq. (27) into the equations of motion (Eqs (22), (23), (24)), we obtain analytical solutions through the following equations where  $\omega$  is the eigenfrequency associated with the  $m^{\text{th}}$  eigenmode, and  $\lambda = m\pi / L$ , as follows:

$$\left( \begin{bmatrix} a_{11} & a_{12} & a_{13} \\ a_{12} & a_{22} & a_{23} \\ a_{13} & a_{23} & a_{33} \end{bmatrix} - \omega^2 \begin{bmatrix} m_{11} & m_{12} & m_{13} \\ m_{12} & m_{22} & m_{23} \\ m_{13} & m_{23} & m_{33} \end{bmatrix} \right) \begin{Bmatrix} U_m \\ W_{bm} \\ W_{sm} \end{Bmatrix} = \begin{Bmatrix} 0 \\ 0 \\ 0 \end{Bmatrix} \tag{28}$$

where

$$a_{11} = A_{11} \lambda^2, \quad a_{12} = -B_{11} \lambda^3, \quad a_{13} = -B_{11}^s \lambda^3 \tag{29}$$

$$a_{22} = D_{11}\lambda^4, \quad a_{23} = D_{11}^s\lambda^4, \quad a_{33} = H_{11}^s\lambda^4 + A_{55}^s\lambda^2 \quad (30)$$

$$m_{11} = I_1, \quad m_{12} = -I_2\lambda, \quad m_{13} = -I_3\lambda \quad (31)$$

$$m_{22} = I_1 + I_4\lambda^2, \quad m_{23} = I_1 + I_5\lambda^2, \quad m_{33} = I_1 + I_6\lambda^2 \quad (32)$$

## 6 RESULTS AND DISCUSSION

### 6.1 Different porosity distribution patterns

Table 1 presents a comparison of various porosity distributions that occur as a result of different fabrication techniques. Porosity refers to the amount of void space or empty volume within a material. It is a measure of how much of the material is made up of empty spaces or pores, relative to the total volume of the material. The distribution of porosity can have a significant impact on the properties and performance of the material, such as strength, durability, and permeability. As shown in Table 1, different fabrication techniques can result in different porosity distributions, and these distributions may be uncertain or difficult to achieve.





Porosity distribution form	Elastic Modulus Expression	Schema
Homogeneous (“H”)	$E(z) = (E_c - E_m) \left( \frac{z}{h} + \frac{1}{2} \right)^k + E_m - (E_c + E_m) \frac{\alpha}{2}$	
“O” shape	$E(z) = (E_c - E_m) \left( \frac{z}{h} + \frac{1}{2} \right)^k + E_m - (E_c + E_m) \frac{\alpha}{2} \left( 1 - 2 \frac{ z }{h} \right)$	
“X” shape	$E(z) = (E_c - E_m) \left( \frac{z}{h} + \frac{1}{2} \right)^k + E_m - (E_c + E_m) \frac{\alpha}{2} \left( 2 \frac{z}{h} \right)$	
“V” shape	$E(z) = (E_c - E_m) \left( \frac{z}{h} + \frac{1}{2} \right)^k + E_m - (E_c + E_m) \frac{\alpha}{2} \left( \frac{1}{2} + \frac{z}{h} \right)$	

Table 1: Different distribution forms of porosity.

The porosity distribution in powder metallurgy depends on several factors such as sintering time, sintering temperature, and reinforcement distribution. Sintering is the process of heating the compacted metal powders to a temperature below the melting point of the metal to fuse the particles together and form a solid, dense component. Sintering time, the duration for which the metal powder is heated at a specific temperature during sintering, is an important parameter as it can affect the microstructure, mechanical properties, and dimensional accuracy of the sintered component. Similarly, sintering temperature can affect the microstructure, mechanical properties, and dimensional accuracy of the sintered component. Porosity can be controlled by adjusting the sintering time and temperature. Longer sintering times and higher sintering temperatures typically lead to lower porosity, while shorter times and lower temperatures result in higher porosity.

The distribution of reinforcement particles can also affect porosity, as the particles can create channels or voids in the material. In centrifugal casting, porosity can occur due to incomplete or improper solidification of the material due to a number of factors. This can happen when the

material cools too quickly, or when there is uneven cooling or solidification due to variations in the casting geometry or mold design.

## 6.2 Validation of the study

Table 2 represents the relationship between frequency and grading parameter  $k$  for a homogeneous porosity distribution, for the case  $L/h = 5$ . The  $L/h$  parameter refers to the length-to-height ratio of the beam structure. In this context, the grading parameter refers to the degree of variation in the material's composition, with higher values of  $k$  indicating a greater variation in composition. The results show that as a general trend, as  $k$  increases, the frequency decreases. This is because metal is stiffer than ceramic and larger values of  $k$  mean that the metal part of material increases over the ceramic part. The method used to generate the results is accurate compared to the results obtained using other methods published in the literature. Table 3 demonstrates the corresponding results for the case  $L/h = 20$ .

Theory	$\alpha$	$k = 0$	$k = 0.2$	$k = 0.5$	$k = 1$	$k = 5$	$k = 10$
CBT*	0	5.3953	5.0206	4.5931	4.1484	3.5949	3.4921
FSDBT*	0	5.1525	4.8066	4.4083	3.9902	3.4312	3.3134
ESDBT*	0	5.1542	4.8105	4.4122	3.9914	3.4014	3.2813
PSDBT*	0	5.1527	4.8092	4.4111	3.9904	3.4012	3.2816
Present	0	5.1529	4.8082	4.4108	3.9906	3.4001	3.2812
	0.1	5.2225	4.8499	4.4044	3.9071	3.1465	3.0284
	0.2	5.3050	4.8998	4.3929	3.7866	2.6946	2.5700

\* Results from Şimşek [28].

Table 2: Variation of fundamental frequency  $\bar{\omega}$  with the power-law index for FG beam for  $L/h = 5$  (Homogeneous distribution form).

Theory	$\alpha$	$k = 0$	$k = 0.2$	$k = 0.5$	$k = 1$	$k = 5$	$k = 10$
CBT*	0	5.4777	5.0967	4.6641	4.2163	3.6628	3.5546
FSDBT*	0	5.4603	5.0827	4.6514	4.2051	3.6509	3.5415
ESDBT*	0	5.4604	5.0829	4.6516	4.2051	3.6483	3.5389
PSDBT*	0	5.4603	5.0829	4.6516	4.2050	3.6485	3.5389
Present	0	5.4603	5.0815	4.6511	4.2051	3.6484	3.5389
	0.1	5.5341	5.1244	4.6413	4.1118	3.3775	3.2808
	0.2	5.6215	5.1755	4.6254	3.9776	2.8855	2.8019

\* Results from Şimşek [28].

Table 3: Variation of fundamental frequency  $\bar{\omega}$  with the power-law index for FG beam for  $L/h = 20$  (Homogeneous distribution form).

## 6.3 Effect of different porosity distributions on natural frequency

It is also worth noting that the presence of porosity in a material can increase the frequency of vibration by providing a cushioning effect. This is because the presence of pores reduces the effective stiffness of the material, which in turn can increase the frequency of vibration. Table 4 presents the results of a frequency analysis for different porosity patterns in a beam structure. The results show that the highest frequency is observed for the homogeneous ("H") type porosity pattern, followed by the "O", "V", and "X" type patterns. Interestingly, for the "X" type pattern, the frequency is higher than for a perfect, non-porous beam. It is important to note that a perfect beam has the lowest frequency in all cases except for the "X" type pattern. This is because a



non-porous beam has no voids or openings for energy to dissipate, resulting in a lower frequency of vibration. The results also indicate that the grading parameter and the  $L/h$  ratio have an impact on the frequency of the beam structure. The grading parameter refers to the variation in porosity within each porosity pattern.

$k$	$L/h$	Porosity distribution patterns				
		Perfect ( $\alpha = 0$ )	“H” ( $\alpha = 0.2$ )	“O” ( $\alpha = 0.2$ )	“X” ( $\alpha = 0.2$ )	“V” ( $\alpha = 0.2$ )
0	5	5.1529	5.3050	5.2888	5.1425	5.2196
	10	5.3933	5.5525	5.5469	5.3812	5.4627
	20	5.4603	5.6215	5.6193	5.4477	5.5305
1	5	3.9905	3.7866	4.0216	4.1574	4.0227
	10	4.1586	3.9364	4.2003	4.3438	4.1954
	20	4.2050	3.9776	4.2499	4.3957	4.2432
5	5	3.4001	2.6946	3.2814	3.6526	3.3603
	10	3.5933	2.8431	3.5035	3.8839	3.5721
	20	3.6483	2.8855	3.5683	3.9506	3.6333
10	5	3.2812	2.5700	3.1520	3.4641	3.2039
	10	3.4814	2.7493	3.4063	3.6920	3.4289
	20	3.5389	2.8019	3.4823	3.7580	3.4947

Table 4: Effect of the shape of porosity distribution on the fundamental frequency  $\bar{\omega}$ .

Figure 2 shows the trend of variation of the frequency with  $L/h$  for different porosity patterns. The porosity pattern refers to the arrangement of the voids within the porous layer, which can greatly affect the properties of the material. The graph shows that for  $L/h > 8$ , the variation in the frequency is not so significant. This means that the material properties have reached a point of saturation and further increasing the  $L/h$  ratio does not significantly affect the frequency. In addition, the “O” and “V” shapes yield very similar results, as shown by the red and blue lines which overlap for most of the graph. This suggests that these two patterns have similar acoustic properties in terms of sound wave frequency variation. Overall, the analysis provides important insights into the behavior of different porous materials and can be useful for designing and selecting materials with porosities.

In both composite materials and FGMs, achieving a uniform distribution of reinforcement material or composition can be difficult. This is because the reinforcement material or composition can have a tendency to clump together or settle out during the manufacturing process. This can result in regions of the material with higher or lower concentrations of reinforcement material or composition, which can have a significant impact on the overall properties of the material. To address this issue, various manufacturing techniques and processes have been developed to ensure a more uniform distribution of reinforcement material or composition. For example, in composite materials, the use of high shear mixing processes, such as ultrasonication or high-speed mixing, can help to disperse the reinforcement material more evenly throughout the matrix material.

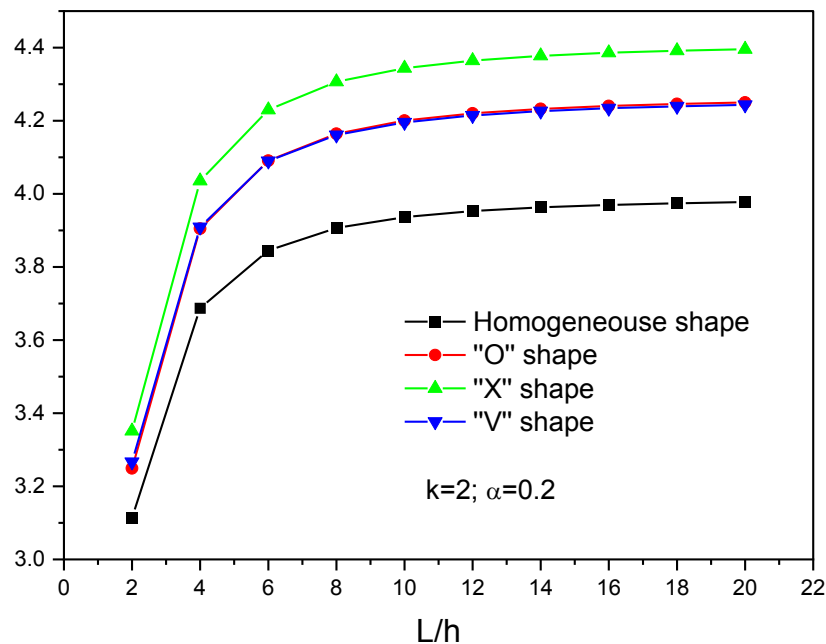


Figure 2. Effect of the shape of porosity distribution on the non-dimensional fundamental frequency  $\bar{\omega}$  versus length-to-thickness ratio  $L/h$  of an  $Al/Al_2O_3$  FGM beam.

## 7 CONCLUSIONS

In composite materials and FGMs, achieving a uniform distribution of reinforcement material or composition can be challenging. Nevertheless, there are various techniques and processes that can be used to improve the uniformity and consistency of these advanced materials. Understanding these factors is important for achieving the desired porosity distribution and ensuring the material has the desired properties and performance. The conducted analysis highlights the importance of porosity distribution and its impact on the properties and performance of materials. The porosity distribution can vary depending on the fabrication technique used and may be difficult to control. The grading parameter and  $L/h$  ratio also affect the frequency of vibration in materials and beam structures, with higher values leading to a decrease in frequency. Porosity can increase the frequency of vibration by providing a cushioning effect, while the arrangement of voids within the porous layer can greatly affect the properties of the material. These findings provide valuable insights into the behavior of different porous materials and can inform the design and selection of materials with specific porosity requirements.

## REFERENCES

- [1] Dev Singh, D., S. Arjula, and A. Raji Reddy, *Functionally Graded Materials Manufactured by Direct Energy Deposition: A review*. Materials Today: Proceedings, 2021. **47**: p. 2450-2456 DOI: <https://doi.org/10.1016/j.matpr.2021.04.536>.
- [2] Jamshidi, M. and J. Arghavani, *Optimal material tailoring of functionally graded porous beams for buckling and free vibration behaviors*. Mechanics Research Communications, 2018. **88**: p. 19-24 DOI: <https://doi.org/10.1016/j.mechrescom.2018.01.006>.

- [3] Suresh, S. and A. Mortensen, *Functionally graded metals and metal-ceramic composites: Part 2 Thermomechanical behaviour*. International Materials Reviews, 1997. **42**(3): p. 85-116 DOI: <https://doi.org/10.1179/imr.1997.42.3.85>.
- [4] Nie, G. and Z. Zhong, *Dynamic analysis of multi-directional functionally graded annular plates*. Applied Mathematical Modelling, 2010. **34**(3): p. 608-616 DOI: <https://doi.org/10.1016/j.apm.2009.06.009>.
- [5] Kermani, I.D., M. Ghayour, and H.R. Mirdamadi, *Free vibration analysis of multi-directional functionally graded circular and annular plates*. Journal of Mechanical Science and Technology, 2012. **26**(11): p. 3399-3410 DOI: <https://doi.org/10.1007/s12206-012-0860-2>.
- [6] Yas, M.H. and N. Moloudi, *Three-dimensional free vibration analysis of multi-directional functionally graded piezoelectric annular plates on elastic foundations via state space based differential quadrature method*. Applied Mathematics and Mechanics, 2015. **36**(4): p. 439-464 DOI: <https://doi.org/10.1007/s10483-015-1923-9>.
- [7] Alipour, M.M., M. Shariyat, and M. Shaban, *A semi-analytical solution for free vibration of variable thickness two-directional-functionally graded plates on elastic foundations*. International Journal of Mechanics and Materials in Design, 2010. **6**(4): p. 293-304 DOI: <https://doi.org/10.1007/s10999-010-9134-2>.
- [8] Nie, G.J. and R.C. Batra, *Stress analysis and material tailoring in isotropic linear thermoelastic incompressible functionally graded rotating disks of variable thickness*. Composite Structures, 2010. **92**(3): p. 720-729 DOI: <https://doi.org/10.1016/j.compstruct.2009.08.052>.
- [9] Shariyat, M. and R. Jafari, *A micromechanical approach for semi-analytical low-velocity impact analysis of a bidirectional functionally graded circular plate resting on an elastic foundation*. Meccanica, 2013. **48**(9): p. 2127-2148 DOI: <https://doi.org/10.1007/s11012-013-9729-4>.
- [10] Eltahir, M.A., et al., *Modified porosity model in analysis of functionally graded porous nanobeams*. Journal of the Brazilian Society of Mechanical Sciences and Engineering, 2018. **40**(3): p. 141 DOI: <https://doi.org/10.1007/s40430-018-1065-0>.
- [11] Abdalla, H.M.A. and D. Casagrande, *An Intrinsic Material Tailoring Approach for Functionally Graded Axisymmetric Hollow Bodies Under Plane Elasticity*. Journal of Elasticity, 2021. **144**(1): p. 15-32 DOI: <https://doi.org/10.1007/s10659-021-09822-y>.
- [12] Bobbio, L.D., et al., *Analysis of formation and growth of the  $\sigma$  phase in additively manufactured functionally graded materials*. Journal of Alloys and Compounds, 2020. **814**: p. 151729 DOI: <https://doi.org/10.1016/j.jallcom.2019.151729>.
- [13] Verma, R.K., D. Parganiha, and M. Chopkar, *A review on fabrication and characteristics of functionally graded aluminum matrix composites fabricated by centrifugal casting method*. SN Applied Sciences, 2021. **3**(2): p. 227 DOI: <https://doi.org/10.1007/s42452-021-04200-8>.
- [14] Mallick, A., S. Gangi Setti, and R.K. Sahu, *Centrifugally cast A356/SiC functionally graded composite: Fabrication and mechanical property assessment*. Materials Today: Proceedings, 2021. **47**: p. 3346-3351 DOI: <https://doi.org/10.1016/j.matpr.2021.07.155>.
- [15] Alshorbagy, A.E., M.A. Eltahir, and F.F. Mahmoud, *Free vibration characteristics of a functionally graded beam by finite element method*. Applied Mathematical Modelling, 2011. **35**(1): p. 412-425 DOI: <https://doi.org/10.1016/j.apm.2010.07.006>.
- [16] Banerjee, J.R., *Dynamic Stiffness Formulation and Free Vibration Analysis of Centrifugally Stiffened Timoshenko Beams*. Journal of Sound and Vibration, 2001. **247**(1): p. 97-115 DOI: <https://doi.org/10.1006/jsvi.2001.3716>.

- [17] Pradhan, K.K. and S. Chakraverty, *Generalized power-law exponent based shear deformation theory for free vibration of functionally graded beams*. Applied Mathematics and Computation, 2015. **268**: p. 1240-1258 DOI: <https://doi.org/10.1016/j.amc.2015.07.032>.
- [18] Vu, T.-V., et al., *Buckling analysis of the porous sandwich functionally graded plates resting on Pasternak foundations by Navier solution combined with a new refined quasi-3D hyperbolic shear deformation theory*. Mechanics Based Design of Structures and Machines, 2022: p. 1-27 DOI: <https://doi.org/10.1080/15397734.2022.2038618>.
- [19] Plevris, V. and G. Tsiatas, *Computational Structural Engineering: Past Achievements and Future Challenges*. Frontiers in Built Environment, 2018. **4**(21): p. 1-5 DOI: <https://doi.org/10.3389/fbuil.2018.00021>.
- [20] Hadji, L., V. Plevris, and R. Madan, *A Static and Free Vibration Analysis of Porous Functionally Graded Beams*, in *2nd International Conference on Civil Infrastructure and Construction (CIC 2023)*. 2023: Doha, Qatar.
- [21] Wattanasakulpong, N. and A. Chaikittiratana, *Flexural vibration of imperfect functionally graded beams based on Timoshenko beam theory: Chebyshev collocation method*. Meccanica, 2015. **50**(5): p. 1331-1342 DOI: <https://doi.org/10.1007/s11012-014-0094-8>.
- [22] Demirhan, P.A. and V. Taskin, *Bending and free vibration analysis of Levy-type porous functionally graded plate using state space approach*. Composites Part B: Engineering, 2019. **160**: p. 661-676 DOI: <https://doi.org/10.1016/j.compositesb.2018.12.020>.
- [23] Wattanasakulpong, N. and V. Ungbhakorn, *Linear and nonlinear vibration analysis of elastically restrained ends FGM beams with porosities*. Aerospace Science and Technology, 2014. **32**(1): p. 111-120 DOI: <https://doi.org/10.1016/j.ast.2013.12.002>.
- [24] Atmane, H.A., et al., *A computational shear displacement model for vibrational analysis of functionally graded beams with porosities*. Steel and Composite Structures, 2015. **19**(2): p. 369-385 DOI: <https://doi.org/10.12989/scs.2015.19.2.369>.
- [25] Hadj, B., B. Rabia, and T.H. Daouadji, *Influence of the distribution shape of porosity on the bending FGM new plate model resting on elastic foundations*. Structural Engineering and Mechanics, 2019. **72**(1): p. 61-70 DOI: <https://doi.org/10.12989/sem.2019.72.1.061>.
- [26] Hadji, L., T.H. Daouadji, and E.A. Bedia, *A refined exponential shear deformation theory for free vibration of FGM beam with porosities*. Geomechanics and Engineering, 2015. **9**(3): p. 361-372 DOI: <https://doi.org/10.12989/gae.2015.9.3.361>.
- [27] Reddy, J.N., *Energy Principles and Variational Methods in Applied Mechanics*. 3rd ed. 2017: Wiley, ISBN: 978-1-119-08737-3.
- [28] Şimşek, M., *Fundamental frequency analysis of functionally graded beams by using different higher-order beam theories*. Nuclear Engineering and Design, 2010. **240**(4): p. 697-705 DOI: <https://doi.org/10.1016/j.nucengdes.2009.12.013>.